International Journal of Pure and Applied Mathematics
Volume 41 No. 9 2007, 1219-1260

SCIENTIFIC VISUALIZATION FOR PDES OF 2ND ORDER I: PROBLEM SETTING AND DATA GENERATION

Lubomir Dechevsky[1 §], Joakim Gundersen[2]
[1,2]R&D Group for Mathematical Modelling
Numerical Simulation and Computer Visualization
Institute for Information, Energy and Space Technology
Narvik University College
2, Lodve Lange's St., P.O. Box 385, Narvik, N-8505, NORWAY
[1]e-mail: ltd@hin.no
[1]url: http://ansatte.hin.no/ltd/
[2]e-mail: joag@hin.no
[2]url: http://ansatte.hin.no/joag/

Abstract: In [9] we studied the geometric, computational and simulation aspects typical for the visualization of the output of simulators of large and complex ODE-based models of dynamical systems (concretely considering the testbed BedSim of the Swedish company LKAB). In a follow-up sequence of 4 papers (of which this is the first one, and [6]-[8] are the other three), we extend the study in [9] to the scientific visualization of Green's functions and solutions of initial-value and boundary-value problems for PDEs of 2nd order, by making graphical comparisons for the elliptic, parabolic and hyperbolic case. We apply the knowledge thus accumulated for the three distinct types, together with a celebrated theorem of Lars Hörmander ([10], [11]), to get geometric insight into the behaviour of solutions of initial-value and boundary-value problems of mixed types. The present article is dedicated to the problem setting and the generation of synthetic data sets used for the visualization results announced in [6]-[8] and for the analysis therein.

AMS Subject Classification: 65M05, 65N05, 68U05, 68U20, 76M27, 34C30, 35A21, 35A40, 35B05, 35B30, 35B35, 35B65, 35C15, 35E05, 35J15, 35J25, 35K05, 35K10, 35K20, 35L05, 35L10, 35L15, 35L20, 35M05, 35M10, 35R05,

Received: November 11, 2007

§Correspondence author

37M05, 65D17, 65D18, 65M06, 65M10, 65M12, 65M15, 65N10, 65N12, 65N15, 65N20, 68U01, 68U07, 68U10, 68U99
Key Words: modelling, simulation, scientific visualization, differential equation, ordinary, partial, dynamical system, initial value, boundary value, finite difference scheme, stability, convergence, error, smooth, fractal, elliptic, parabolic, hyperbolic, mixed-type, propagation of singularities, Green's function, fundamental solution, continual, discrete, isocurve, isosurface, colour map, computational geometry, computer-aided geometric design, computer graphics, applied mathematics

1. Introduction

In a sequence of 4 papers, of which this is the first one, followed by [6], [7], [8], we study on several model initial and boundary value problems for partial differential equations (PDEs), various aspects of *scientific visualization* (see, e.g., [18]) as a central part of the verification of the results obtained in the process of modelling and simulation of dynamical systems, as described in the flowchart on Figure 1. One important reason for the central role of visualization in the verification and validation of the process of modelling and simulation is due to the fact that, in average, considerably more than half of the total information exchange of the human brain with the external environment is carried through the visual cortex and other zones of the brain associated with visual data processing. "The best connection between humans and computers is through the high-bandwidth connection of our highly evolved visual system" – Wes Bethel [1].

Our interest in Scientific visualization related to PDEs stemmed from an applied mathematics research project of the Priority R&D Group for Mathematical Modelling, Numerical Simulation and Computer Vizualization (the R&D Simulations Group, for short) at Narvik University College, of which both authors are members. Our industrial partner in this joint research project was the R&D Department of LKAB (www.lkab.com), an international high-tech iron ore processing company seated in Kiruna in Northern Sweden.

Our task in this research project was to develop methods and software for animated 4D space-time visualization of the "warm part" of the iron-pellets production process, as modelled in LKAB's own simulator developed in the course of the last 27 years, BedSim.

The simulation in BedSim is based on a model of a 64-parameter time-

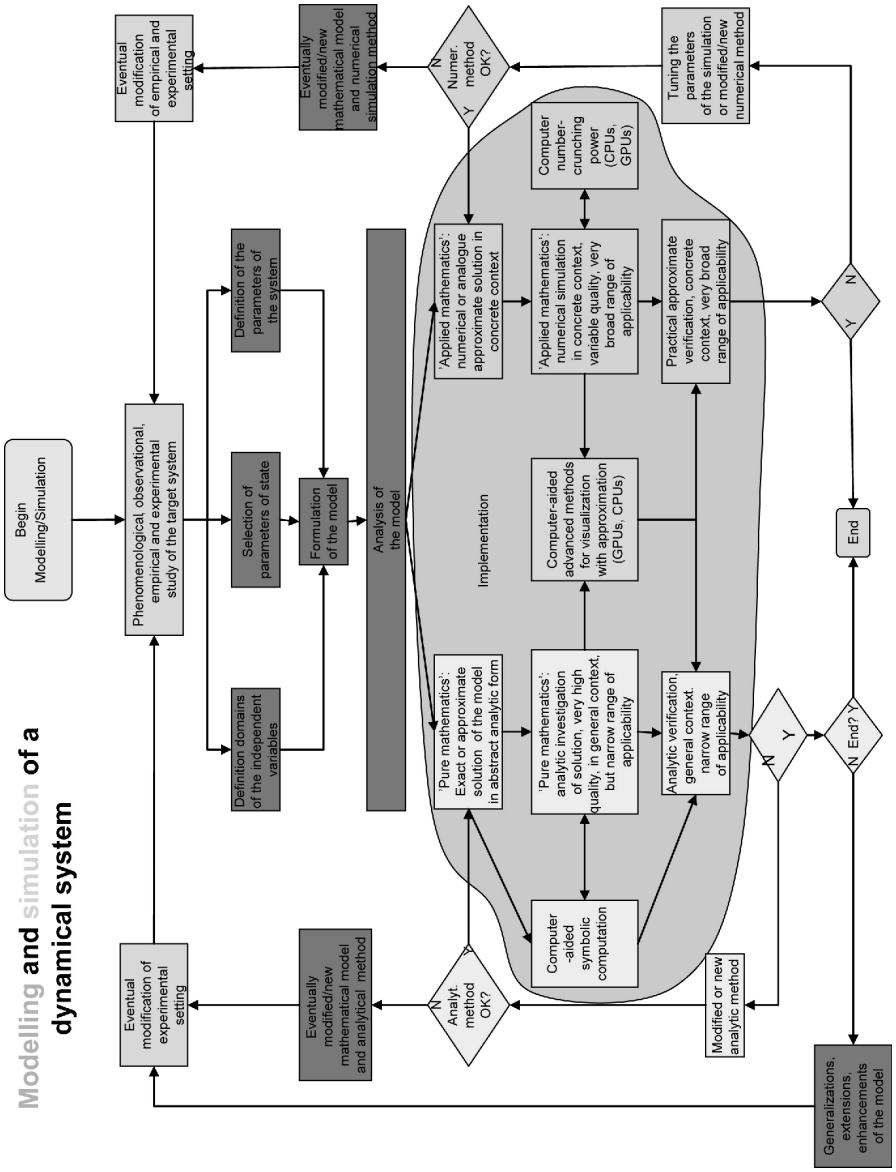

Figure 1: Flowchart of the process of modelling and simulation of a dynamical system, by Lubomir Dechevsky, used in the course STE6239 Simulations at Narvik University College. This flowchart is an extension and upgrade of Scheme 1.1 in [12].

dependent dynamical system described by a large system of non-linear ordinary differential equations (ODEs). In [9] we discussed the generation of multidimensional time-dependent geometric data sets from the numerical output of BedSim and provided model results of their scientific visualization using our in-house software application, developed within the doctoral project of the second author, financed by R&D LKAB and the Norwegian government and supervised by the first author. (See the next section for more details about our software implementation.)

In the concluding section of [9] we discussed the limitations of the current ODE-system-based testbed version of BedSim and the necessity to upgrade it to a PDE-based testbed version in the future. Certain mathematical and visualization aspects of this upgrade lead us to the study described in the present article and the follow-up sequence of articles [6], [7] and [8].

Two of the observations we made about BedSim in the concluding section of [9] were, as follows:

1. Rather than using a high-dimensional system of (generally, nonlinear) ODEs in part of the BedSim model, use low-dimensional system of (nonlinear) PDEs.

2. LKAB is particulary interested in preventing certain critical phenomena from happening during the warm part of their industrial process; we conjectured that these phenomena have relevance to sharp changes, including discontinuities, in the coefficients of the PDE in item 1, leading to discontinuous changes in the properties of the solution, partially due to the local change of type of the PDE.

In the next section we briefly describe the visualization methods and the software tools we propose to use in relation to items 1. and 2. above.

2. Visualization Methods and Tools

In [6], [7], [8] we shall use the following approaches to visualization:

1. Visualization in 3D of geometric objects which can be immersed in 2D and 3D. This is the orthodoxal way of viewing geometric objects in 3-dimensional virtual universes (we use OpenGL for this purpose).

2. Visualization in 2D of geometric objects immersed in nD, where n may be 1, 2, 3 but also it is possible that $n \geqq 4$.

   (a) Colour (mode 1) visualization (see [5]). We use it to describe real scalar values. The scaled value corresponds to an appropriately scaled colour in the visible part of the light spectrum. In the place of colour, a more economical grey-scale representation suffices: the scaled value corresponds to the scaled intensity of grey (say, "larger value" corresponds to "lighter grey").

   (b) Colour (mode 2) visualization (see [5]). Used to represent vector values for dimension of the vector up to 3 (say, scaled values of x, y and z); corresponds to intensity of red, green and blue, respectively, in the RGB colour system. It can be used also for visualization in 4D of the graph of a complex-valued function of one complex variable (see [13]).

   (c) Colour (mode 3) visualization (see [5]). An advanced method for representation of n-dimensional geometric objects as colour or grey-scale images in 2D using (bi)orthonormal wavelets, first proposed in [4], [5]. (In the notation of [5], the grey-scale version of the mode 3 mapping is denoted as mode 3.1, while the RGB-colour version of the mode 3 mapping is denoted as mode 3.2).

For further information we refer to [5]. Some of the applications of the visualization techniques in item 2(a) and, especially, (b) and (c), are related to GPU-programming, see [5].

For the visualization in [6], [7], [8] we shall use our in-house software application described in [9]. It is based on .NET2005 (C++), OpenGL, together with our in-house libraries GM_Lib (for geometric modelling) and GM_Waves (for wavelet processing), and Trolltech Qt for the user interface.

3. Problem Setting

Our purpose in this article and in [6], [7], [8] is to study how our visualization application developed for visualization of the numerical output of the ODE-based testbed BedSim works on data sets generated from PDEs and their numerical approximations. We shall consider first the model examples of the 3 basic types of 2nd order linear PDEs with constant real coefficients and variable right-hand

side (RHS): parabolic, hyperbolic and elliptic PDE for initial and boundary-value problems on the rectangle $\{(x,t) : x \in [0,1], t \in [0,T], 0 < T < \infty\}$, that is, the space variable x will be 1D. We shall use the same model RHS for all examples of the 3 types of equations. Wherever possible, we shall use also the same model initial/boundary-value functions. Under these comparable conditions, we shall visualize:

- The exact (continual) Green's function for the boundary problem for the respective PDE (using isosurfaces in 3D and colour (mode 3) maps in 5D) computed with high precision from its closed-form analytical representation. (Because the Green's function has singularities, in this computation we use a simple quadrature rule (typically, trapezoid) with a very small step.) See [6].

- The exact (continual) solution of the boundary problem for the respective PDE, computed by high-precision numerical-quadrature approximation of the closed-form integral representation of the solution. (We consider only very smooth RHS and initial/boundary-value functions, so that it is easy to obtain high convergence rates in the quadrature approximation. In this case, we use higher-order quadrature formulae, with a larger step – typically, accelerating the convergence by several iterations of Richardson extrapolation (Runge principle) via Romberg integration starting from the trapezoid rule.) We shall use visualization as a functional surface in 3D and colour (mode 1) maps. See [7].

For the parabolic equation, we consider also the discrete approximation by classical 2-layer difference schemes (see [15]). These difference schemes depend on the step h in the 1D space variable x, τ in the time variable t, and on $\sigma \in [0,1]$ where the parameter σ provides a quantitative measure of the implicitness of the difference scheme ($\sigma = 0$ corresponds to the "purely" explicit scheme, and $\sigma = 1$ corresponds to the "purely" implicit scheme (see [15])).

It is known (see [15], Section 5.1.3–5.1.7) that this type of difference schemes are stable (in appropriate mesh-dependent norms, both with respect to initial data and to RHS and boundary-value data) when the steps h and τ are related with σ by

$$0 \leq \sigma_0 \leq \sigma \leq 1, \tag{1}$$

where σ_0 is σ_ε for $\varepsilon = 0$ in the expression $\sigma_\varepsilon = \frac{1}{2} - \frac{1-\varepsilon}{4\tau}h^2$, $0 \leq \varepsilon \leq 1$. It is also known that, in general, for every σ satisfying (1) the rate of local approximation of this difference scheme is $O(h^2 + \tau)$, but in the special case $\sigma = \frac{1}{2} = \sigma_\varepsilon$ for

$\varepsilon = 1$ the rate of approximation improves for $O^(h^2 + \tau^2)$, and in the special case

$$\sigma^* = \frac{1}{2} - \frac{h^2}{12\tau} = \sigma_\varepsilon, \quad \text{for} \quad \varepsilon = \frac{2}{3}$$

the difference scheme has increased rate of local approximation $O(h^4 + \tau^2)$ for appropriately chosen RHS of the difference scheme, if the RHS in (2) below is sufficiently smooth (see [15], Section 5.1.3). Moreover, the schemes with $\sigma = \frac{1}{2}$, σ^* are stable, since it is easy to see that $\sigma = \frac{1}{2}$, $\sigma = \sigma^*$ satisfies (1).

Taking these facts into consideration, we shall visualize:

- The error of approximation of the exact continual Green's function by the discrete Green's function for fixed h, τ and varying σ (when (1) is fulfilled) with special attention to the boundary case between stability and instability, $\sigma = \sigma_0$, which is stable but interesting additional phenomena are observed due to the numerical round-up errors. Namely:
  - For the limiting case of stability $\sigma = \sigma_0$ the error manifold has fractal geometry, because the numerical round-up errors act like noise.
  - For $\sigma > \sigma_0$ the error manifold smooths out, that is, the increase of σ above the critical σ_0 has denoising effect and, in this context, the parameter $\sigma - \sigma_0$ takes the role of a Tikhonov-regularization small parameter.

  For this visualization we shall use isosurfaces in 3D and colour (mode 3) maps. See [8].

- For several representative values of σ (including both stable and unstable cases), the error of approximation on the mesh of the exact continual solution of the boundary problem by the discrete solution of the finite difference scheme (visualized as a functional surface in 3D and via a colour (mode 1) map). See [8].

After studying the basic cases of linear PDE with constant coefficients of elliptic, parabolic and hyperbolic type, we return to the context of BedSim. Based on our experience with visualization of the data sets generated via the present ODE-based version of BedSim, we conjecture that a PDE upgrade of its model should involve possible discontinuities in the PDE coefficients and non-linear terms, including possibly cases when the type of PDEs changes locally in space and time. For example, such effects may be due to local spontaneous exothermic or endothermic chemical reactions accompanied by possible local

changes of aggregate phase (e.g., from liquid to gas) – see also [9]. Our experience also suggests that our real-time visualization algorithms and software make possible the visual detection and recognition of such zones of special effects. We demonstrate this approach on two simple model examples of boundary problems for mixed-type PDEs by comparing the singularities of their solutions using graphical visualization and an argument based on a celebrated theorem of Lars Hörmander ([10], [11], Theorems 24.5.3 and 24.5.4). See [7].

The organization of the remaining part of this paper is, as follows.

In Section 4 we provide a rigorous description of the data sets used as input to our visualization software for the considered boundary problems for PDEs. Subsections 4.1, 4.2, 4.3 are dedicated to the continual Green's functions and solutions of the parabolic, hyperbolic and elliptic PDEs, respectively. Subsection 4.4 deals with the discrete Green's function and the discrete solution of the finite difference scheme for the parabolic PDE. The derivations of the respective formulae can only be collected in small bits (for different boundary problems) from a relatively large number of reference sources. For the reader's convenience, and since we want to compare the solutions of the elliptic and hyperbolic equation for comparable boundary data and RHS, we have included a brief self-contained exposition of the respective derivations in Appendices A-D.

4. Generating the Data Sets

4.1. The Parabolic Equation

We consider the continual initial and boundary-value problem for the one dimensional scaled parabolic PDE:

$$\begin{array}{ll} \dfrac{\partial u}{\partial t}(x,t) - \dfrac{\partial^2 u}{\partial x^2}(x,t) = F(x,t), & (x,t)\epsilon[0,1]\times[0,T] \\ u(x,0) = \phi(x), & x \in [0,1] \\ u(0,t) = \psi^{(0)}(t),\ u(1,t) = \psi^{(1)}(t), & t \in [0,T] \end{array} \tag{2}$$

with the consistency conditions $\phi(0) = u(0,0) = \psi^{(0)}(0)$, $\phi(1) = u(1,0) = \psi^{(1)}(0)$.

Some of the formulae in this subsection can be collected from numerous classical reference sources, such as [17] or [16]. A detailed derivation of all formulae is given in Appendix A.

4.1.1. Green's Function

The Green's function for problem 2 is given by

$$\begin{aligned} G(x,\xi;t,\tau) &= G(x,\xi;t-\tau) \\ &= 2\sum_{n=1}^{\infty} e^{-\pi^2 n^2 (t-\tau)} \sin(\pi n x) \sin(\pi n \xi) \end{aligned} \tag{3}$$

The proof of (3) is given in Appendix A.1.

4.1.2. Integral Representation of the Exact Solution of (2)

The solution $u(x,t)$ of (2) can be written in closed integral form, as follows:

$$\begin{aligned} u(x,t) = &\int_0^t \int_0^1 G(x,\xi;t-\tau)\cdot F(\xi,\tau)d\xi d\tau \\ &+ \int_0^1 G(x,\xi;t)\cdot\varphi(\xi)d\xi \\ &+ \int_0^t \frac{\partial}{\partial\xi} G(x,0;t-\tau)\cdot\psi^{(0)}(\tau)d\tau \\ &- \int_0^t \frac{\partial}{\partial\xi} G(x,1;t-\tau)\cdot\psi^{(1)}(\tau)d\tau \end{aligned} \tag{4}$$

(The derivatives $\frac{\partial}{\partial\xi}G$ and $-\frac{\partial}{\partial\xi}G$ correspond to the normal derivative on the respective part of the boundary.)

Formula (4) contains singular integrals and is valid also in the case of non-smooth initial and boundary-value data functions. However, for this general case, the quadrature formulae by means of which we shall approximate the integrals in (4) (in order to generate the discrete data input into our visualization software) may be very slowly convergent. Therefore, we shall use only sufficiently smooth initial and boundary-value data functions, when (4) can be

replaced by the equivalent representation

$$\begin{aligned} u(x,t) = &\int_0^t \int_0^1 G\left(x,\xi;t-\tau\right)\cdot \bar{F}\left(\xi,\tau\right) d\xi d\tau \\ &+ \int_0^1 G\left(x,\xi;t\right)\cdot \bar{\Phi}\left(\xi\right) d\xi \\ &+ \left(1-x\right)\cdot \psi^{(0)}\left(t\right) + x\cdot \psi^{(1)}\left(t\right) \end{aligned} \tag{5}$$

where

$$\bar{F}\left(\xi,\tau\right) = F\left(\xi,\tau\right) - \left(1-\xi\right)\cdot \dot{\psi}^{(0)}\left(\tau\right) - \xi\cdot \dot{\psi}^{(1)}\left(\tau\right)$$
$$\bar{\Phi}\left(\xi\right) = \varphi\left(\xi\right) - \left(1-\xi\right)\cdot \psi^{(0)}\left(0\right) - \xi\cdot \psi^{(1)}\left(0\right)$$

For a proof of (5) and deriving (4) from there, see Appendix A.2.

4.2. The Hyperbolic Equation

We consider the continual initial and boundary-value problem for the one dimensional scaled hyperbolic PDE:

$$\begin{array}{ll} \dfrac{\partial^2 u}{\partial t^2}(x,t) - \dfrac{\partial^2 u}{\partial x^2}(x,t) = F(x,t), & (x,t)\epsilon[0,1]\times[0,T] \\ u(x,0) = \varphi^{(0)}(x), & x\epsilon[0,1] \\ \frac{\partial u}{\partial t}(x,0) = \varphi^{(1)}(x), & x\epsilon[0,1] \\ u(0,t) = \psi^{(0)}(t),\ u(1,t) = \psi^{(1)}(t), & t\epsilon[0,T] \end{array} \tag{6}$$

with the consistency conditions $\varphi^{(0)}(0) = u(0,0) = \psi^{(0)}(0)$, $\varphi^{(0)}(1) = u(1,0) = \psi^{(1)}(0)$.

Some of the formulae in this subsection can be collected from numerous classical reference sources, such as [17] or [16]. A detailed derivation of all formulae is given in Appendix B.

4.2.1. Green's Function

The Green's function for problem 6 is given by

$$G\left(x,\xi;t\right) = \frac{2T}{\pi}\sum_{n=1}^{\infty}\frac{1}{n}\cdot \sin\left(\frac{\pi n t}{T}\right)\cdot \sin\left(\pi n x\right)\cdot \sin\left(\pi n \xi\right) \tag{7}$$

The proof of (7) is given in Appendix B.1.

4.2.2. Integral Representation of the Exact Solution of (6)

The solution $u(x,t)$ of (6) can be written in closed integral form, as follows:

$$\begin{aligned} v(t) = & \int_0^t \int_0^1 G\left(x,\xi;t-\tau\right)\cdot F\left(\xi,\tau\right)d\xi d\tau \\ & + \int_0^1 G_t\left(x,\xi;t\right)\cdot\varphi^{(0)}\left(\xi\right)d\xi + \int_0^1 G\left(x,\xi;t\right)\cdot\varphi^{(1)}\left(\xi\right)d\xi \\ & + \int_0^t G_\xi\left(x,0;t-\tau\right)\cdot\psi^{(0)}\left(\tau\right)d\tau - \int_0^1 G_\xi\left(x,1;t-\tau\right)\cdot\psi^{(1)}\left(\tau\right)d\tau \end{aligned} \tag{8}$$

Formula (8) contains singular integrals and is valid also in the case of non-smooth initial and boundary-value data functions. However, for this general case, the quadrature formulae by means of which we shall approximate the integrals in (8) (in order to generate the discrete data input into our visualization software) may be very slowly convergent. Therefore, we shall use only sufficiently smooth initial and boundary-value data functions, when (8) can be replaced by the equivalent representation

$$\begin{aligned} u(x,t) = & \int_0^t \int_0^1 G\left(x,\xi;t-\tau\right)\cdot\bar{F}\left(\xi,\tau\right)d\xi d\tau \\ & + \int_0^1 G_t\left(x,\xi;t\right)\cdot\bar{\Phi}^{(0)}\left(\xi\right)d\xi + \int_0^1 G\left(x,\xi;t\right)\cdot\bar{\Phi}^{(1)}\left(\xi\right)d\xi \\ & + (1-x)\cdot\psi^{(0)}\left(t\right) + x\cdot\psi^{(1)}\left(t\right) \end{aligned} \tag{9}$$

where

$$\begin{aligned} \bar{F}\left(\xi,\tau\right) &= F\left(\xi,\tau\right) - (1-\xi)\cdot\ddot{\psi}^{(0)}\left(\tau\right) - \xi\cdot\ddot{\psi}^{(1)}\left(\tau\right) \\ \bar{\Phi}^{(0)}\left(\xi\right) &= \varphi^{(0)}\left(\xi\right) - (1-\xi)\cdot\psi^{(0)}\left(0\right) - \xi\cdot\psi^{(1)}\left(0\right) \\ \bar{\Phi}^{(1)}\left(\xi\right) &= \varphi^{(1)}\left(\xi\right) - (1-\xi)\cdot\dot{\psi}^{(0)}\left(0\right) - \xi\cdot\dot{\psi}^{(1)}\left(0\right) \end{aligned}$$

For a proof of (9) and deriving (8) from there, see Appendix B.2.

4.3. The Elliptic Equation

We consider the continual boundary-value problem for the one dimensional scaled elliptic PDE:

$$\begin{array}{ll} \dfrac{\partial^2 u}{\partial t^2}(x,t) + \dfrac{\partial^2 u}{\partial x^2}(x,t) = F(x,t), & (x,t)\epsilon[0,1]\times[0,T] \\ u(x,0) = \varphi^{(0)}(x), & x\epsilon[0,1] \\ u(x,T) = \varphi^{(1)}(x), & x\epsilon[0,1] \\ u(0,t) = \psi^{(0)}(t),\ u(1,t) = \psi^{(1)}(t), & t\epsilon[0,T] \end{array} \tag{10}$$

with the consistency conditions $\varphi^{(0)}(0) = \psi^{(0)}(0)$, $\varphi^{(0)}(1) = \psi^{(1)}(0)$, $\varphi^{(1)}(0) = \psi^{(0)}(T)$ and $\varphi^{(1)}(1) = \psi^{(1)}(T)$.

Note that, unlike the case of the hyperbolic equation, here we do not consider the initial and boundary value problem in (6). One reason is that in the elliptic equation the variables x and t play a symmetric role, and we thus prefer to look at (x,t) as a two-dimensional space variable, rather than a pair of a space and time variable. Another reason is that initial and boundary value in (8) translates into a mixed Dirichlet - Neumann boundary value problem for the elliptic equation where Dirichlet data are given on part of the boundary, and Neumann data are given on the remaining part of this boundary. Instead, we prefer to study here the simpler Dirichlet boundary value problem (10) where the data on the whole boundary are of Dirichlet type. In this case the necessary formulae for the Green's function can be collected from [16], and the derivation of the integral representation of the solution can be done along the lines of a part of the respective derivation for the hyperbolic equation (see Appendix C).

4.3.1. Green's Function

The Green's function for problem 10 is given by

$$\begin{aligned} &G(x,\xi;t,\tau) = \\ &= 2\sum_{n=1}^{\infty} \frac{\sinh\left(\pi n\cdot\min\{t,\tau\}\right)\sinh\left(\pi n\cdot(1-\max\{t,\tau\})\right)}{\pi n\sinh(\pi n)}\sin(\pi n x)\sin(\pi n\xi) \\ &\qquad\qquad x,\xi,t,\tau\in[0,1]\,. \end{aligned} \tag{11}$$

4.3.2. Integral Representation of the Exact Solution of (10)

The solution $u(x,t)$ of (10) can be written in closed integral form, as follows:

$$\begin{aligned} u(x,t) = & \int_0^t \int_0^1 G(x,\xi;t,\tau)\cdot F(\xi,\tau)\,d\xi d\tau \\ & + \int_0^1 G_\tau(x,\xi;t,0)\cdot\varphi^{(0)}(\xi)d\xi + \int_0^1 G_\tau(x,\xi;t,1)\cdot\varphi^{(1)}(\xi)d\xi \qquad (12) \\ & + \int_0^1 G_\xi(x,0;t,\tau)\cdot\psi^{(0)}(\tau)d\tau - \int_0^1 G_\xi(x,1;t,\tau)\cdot\psi^{(1)}(\tau)d\tau. \end{aligned}$$

where

$$G_\tau(x,\xi,t,0) = 2\sum_{n=1}^{\infty}\frac{\sinh(\pi n(1-t))}{\sinh(\pi n)}\sin(\pi nx)\sin(\pi n\xi)$$

$$G_\tau(x,\xi,t,1) = -2\sum_{n=1}^{\infty}\frac{\sinh(\pi nt)}{\sinh(\pi n)}\sin(\pi nx)\sin(\pi n\xi)$$

$$G_\xi(x,0,t,\tau) = 2\sum_{n=1}^{\infty}\frac{\sinh(\pi n\cdot\min\{t,\tau\})\sinh(\pi n\cdot(1-\max\{t,\tau\}))}{\sinh(\pi n)}\sin(\pi nx)$$

$$G_\xi(x,1,t,\tau) = 2\sum_{n=1}^{\infty}(-1)^n\frac{\sinh(\pi n\cdot\min\{t,\tau\})\sinh(\pi n\cdot(1-\max\{t,\tau\}))}{\sinh(\pi n)}$$

Formula (12) contains singular integrals and is valid also in the case of non-smooth initial and boundary-value data functions. However, for this general case, the quadrature formulae by means of which we shall approximate the integrals in (12) (in order to generate the discrete data input into our visualization software) may be slowly convergent. Therefore, we shall use only sufficiently smooth initial and boundary-value data functions, when (12) can be replaced by the equivalent representation

$$\begin{aligned} u(x,t) = & \int_0^t \int_0^1 G(x,\xi;t,\tau)\cdot\bar{F}(\xi,\tau)\,d\xi d\tau \\ & + \int_0^1 G_\tau(x,\xi;t,0)\cdot\bar{\varphi}^{(0)}(\xi)d\xi + \int_0^1 G_\tau(x,\xi;t,1)\cdot\bar{\varphi}^{(1)}(\xi)d\xi \end{aligned}$$

$$+ (1-x)\cdot\psi^{(0)}(t) + x\cdot\psi^{(1)}(t) + \left(\frac{T-t}{T}\right)\cdot\varphi^{(0)}(x) + \frac{t}{T}\cdot\varphi^{(1)} - \rho(x,t)\,, \quad (13)$$

where

$$\begin{aligned}
\bar{F}(\xi,\tau) =& F(\xi,\tau) - (1-\xi)\cdot\ddot{\psi}^{(0)}(\tau) - \xi\cdot\ddot{\psi^{(1)}}(\tau) \\
&- \left(\frac{T-\tau}{T}\right)\cdot\varphi''^{(0)}(\xi) - \frac{\tau}{T}\cdot\varphi''^{(1)}(\xi), \\
\bar{\varphi}^{(0)}(\xi) =& -(1-\xi)\cdot\psi^{(0)}(0) - \xi\cdot\psi^{(1)}(0) + \rho(\xi,0), \\
\bar{\varphi}^{(1)}(\xi) =& -(1-\xi)\cdot\psi^{(0)}(T) - \xi\cdot\psi^{(1)}(T) + \rho(\xi,T),
\end{aligned}$$

where the remainder $\rho(\xi,\tau)$ can be taken in the following tensor-product form:

$$\begin{aligned}
\rho(\xi,\tau) =& \sum_{\mu=0}^{1}\sum_{\nu=0}^{1} u(\xi_\mu,\tau_\nu) b_\mu(\xi) b_\nu(\tau) \\
=& u(0,0)\cdot(1-\xi)\cdot\left(\frac{T-\tau}{T}\right) + u(0,T)\cdot(1-\xi)\cdot\frac{\tau}{T} \\
&+ u(1,0)\cdot\xi\cdot\left(\frac{T-\tau}{T}\right) + u(1,T)\cdot\xi\cdot\frac{\tau}{T}.
\end{aligned}$$

4.4. Finite Difference Schemes for the Parabolic Equation

To find an approximate solution of (2), we consider the following discrete two-layer finite-difference problem:

$$\begin{gathered}
\frac{V_{ij+1} - V_{ij}}{\tau} \\
- \left(\sigma\frac{V_{i+1j+1} - 2V_{ij+1} + V_{i-1j+1}}{h^2} + (1-\sigma)\frac{V_{i+1j} - 2V_{ij} + V_{i-1j}}{h^2}\right) = f_{ij} \\
i = 1,2,\ldots,N-1, \quad j = 0,1,2,\ldots,M-1 \\
V_{i0} = \phi_i, \qquad i = 0,1,\ldots,N \\
V_{0j} = \psi_j^{(0)}, \quad V_{Nj} = \psi_j^{(1)}, \qquad j = 0,1,\ldots,M
\end{gathered} \quad (14)$$

with the discrete consistency conditions $\phi_0 = V_{00} = \psi_0^0$, $\phi_N = V_{N0} = \psi_0^1$. Here

$$\begin{gathered}
x_i = ih, \quad i = 0,1,\ldots,N, \quad Nh = 1 \\
t_j = j\tau, \quad j = 0,1,\ldots,M, \quad M\tau = T
\end{gathered}$$

For σ we assume $\sigma\epsilon[0,1]$ ($\sigma = 0$ – explicit scheme; $\sigma = \frac{1}{2}$ – Crank-Nicholson (implicit) scheme; $\sigma = 1$ – backward Euler (fully) implicit scheme)

Some of the formulae in this subsection can be collected from [15] and [3]. For detailed derivations, see Appendix D.

4.4.1. Discrete Green's Function

The discrete Green's function for problem (14) is given by

$$G_{ij}^{\nu\mu} = \sum_{n=1}^{N-1} \frac{1}{1+\lambda_n\tau\sigma} \left(1 - \frac{\lambda_n\tau}{1+\lambda_n\tau\sigma}\right)^{j-\mu-1} X_n(x_\nu)X_n(x_i) \tag{15}$$

with respect to the RHS and boundary conditions, and

$$\Gamma_{ij}^{\nu} = \sum_{n=1}^{N-1} \left(1 - \frac{\lambda_n\tau}{1+\lambda_n\tau\sigma}\right)^{j} X_n(x_\nu)X_n(x_i) \tag{16}$$

with respect to the initial condition.

In (15) and (16)

$$\begin{aligned} \lambda_\nu &= \frac{4}{h^2}\sin^2\left(\frac{\pi\nu h}{2}\right) = \frac{4}{h^2}\sin^2\left(\frac{\pi x_\nu}{2}\right) \\ X_\nu &= \sqrt{2}\sin(\pi\nu x_i) \end{aligned}$$

The proof of (15) and (16) is given in Appendix D.1.

4.4.2. Explicit Solution of (14)

We then have this explicit solution of (14)

$$\begin{aligned} V_{ij} &= w_{ij} + (1-x_i)\psi_j^{(0)} + x_i\psi_j^{(1)} \\ &= \sum_{\nu=1}^{N-1} h\Gamma_{ij}^{\nu}\Phi_\nu + \sum_{\mu=0}^{j-1}\sum_{\nu=1}^{N-1} h\tau G_{ij}^{\nu\mu}F_{\nu\mu} + (1-x_i)\psi_j^{(0)} + x_i\psi_j^{(1)} \end{aligned} \tag{17}$$

where

$$F_{ij} = f_{ij+\frac{1}{2}} - \frac{(1-x_i)\left(\psi_{j+1}^{(0)} - \psi_j^{(0)}\right) + x_i\left(\psi_{j+1}^{(1)} - \psi_j^{(1)}\right)}{\tau} \tag{18}$$

$$\Phi_i = \phi_i - (1-x_i)\psi_0^{(0)} - x_i\psi_0^{(1)} \tag{19}$$

The proof of (17) is given in Appendix D.2.

Formulae (17 – 19) are the discrete analogue of (5). By commuting the order of summation and summation by parts in (17), it is possible to obtain from (17 – 19) a direct discrete analogue of (8). We omit this here, since (17 – 19) are sufficient for our visualization purposes.

5. Concluding Remarks

The consistency conditions in initial-/boundary-value problems (2), (6) and (10) (see also the Appendices) can be relaxed so, that these problems still have a unique classical solution. Such is, for example, the case when these consistency conditions do not hold, the solution $u(x,t)$ is possibly discontinuous in some or all of the corners $(0,0)$, $(1,0)$, $(0,T)$, $(1,T)$, the respective one-sided limits $u(0+,0)$, $u(0,0+)$, $u(0+,T)$, $u(0,T-)$, $u(1-,0)$, $u(1,0+)$, $u(1-,T)$, $u(1,T-)$ all exist, and are such that

$$\begin{aligned} u(0,0+)-\psi^{(0)}(0) &= \quad u(0+,0)-\varphi^{(0)}(0) = \quad A_{00} \\ u(0,T-)-\psi^{(0)}(T) &= \quad u(0+,T)-\varphi^{(1)}(0) = \quad A_{01} \\ u(1,0+)-\psi^{(1)}(0) &= \quad u(1-,0)-\varphi^{(0)}(1) = \quad A_{10} \\ u(1,T-)-\psi^{(1)}(T) &= \quad u(1-,T)-\varphi^{(1)}(1) = \quad A_{11} \end{aligned} \tag{20}$$

hold simultaneously. In this case the formula for $\rho(\xi,\tau)$ in (13) is

$$\rho(\xi,\tau)=\sum_{\mu=0}^{1}\sum_{\nu=0}^{1}A_{\mu\nu}b_{\mu}(\xi)b_{\nu}(\tau). \tag{21}$$

The integral representations of the solutions (4), (8) and (12) are derived in the Appendix only for sufficiently smooth data (RHS, initial-values and boundary-values) of the initial-/boundary-value problem, because these formulae are obtained from (5), (9) and (13), respectively, which are valid only for sufficiently smooth data. In fact (4), (8) and (12) can be appropriately extended for less regular, even distributional, data by using a very general standard continuity/density argument which is described, e.g., in [14], Chapter I, Theorem 7. The full analysis and technical details of this standard argument will not be discussed explicitly in this paper or the sequence of papers [6]-[8].

It is also possible to make the high-precision computation of the Green's functions more efficient, by using adaptive quadratures. This is relatively easy to do, since it is known exactly where the Green's functions have singularities (and these singularities are of the simple 'split diagonal' type).

There is rich diversity of topics for further work on scientific visualization in the field of PDEs and their solutions. Here we give only one simple special topic and one advanced general topic, as follows.

- In the error visualization in [8], it is of considerable interest to study and visualize also the error distribution for the scheme with higher rate of local approximation $O(h^4+\tau^2)$ for $\sigma=\sigma^*=\sigma_{\frac{2}{3}}=\frac{1}{2}\left(1-\frac{h^2}{6\tau}\right)$ and

special RHS in (17)-(19), where F_{ij} in (18) should be replaced by

$$\tilde{F}_{ij} = \frac{5}{6}F_{ij} + \frac{1}{12}\left(F_{i-1,j} + F_{i+1,j}\right) \tag{22}$$

(see [15], Section 5.1.3).

- Of great interest is the visualization of the error distribution for iterative methods of approximate solution of non-linear ODEs and PDEs.

Acknowledgements

This work was supported in part by the 2003, 2004, 2005, 2006 and 2007 Annual Research Grants of the priority R&D Group for Mathematical Modeling, Numerical Simulation and Computer Visualization at Narvik University College, Norway.

The work of the second of the two authors was also partially supported by a doctoral fellowship grant from LKAB, Sweden (http://lkab.com/).

References

[1] W. Bethel, Parallelism in Graphics and Visualization, A Lecture for the CS267 Course "Applications of Parallel Computers", Spring 2006, Presentation of the Visualization Group at the Ernest Orlando Lawrence Berkeley National Laboratory, http://www-vis.lbl.gov/Presentation.

[2] M. Carter, B. van Brunt, *The Lebesgue-Stieltjes Integral*, Undergraduate Texts in Mathematics, Springer-Verlag, New York (2000).

[3] L.T. Dechevsky, *Some Applications of the Theory of Function Spaces in Numerical Analysis*, Ph.D. Dissertation, Sofia University, Sofia (1989), In Bulgarian.

[4] L.T. Dechevsky, J. Gundersen, From dynamical visualization of large 3D and 4D geometrical data sets to isometric conversion between dimension and resolution, *Applied Mathematics*, Narvik University College, Narvik, Norway, No. 3 (2004), Preprint Series ISSN 1504-4653.

[5] L.T. Dechevski, J. Gundersen, Isometric conversion between dimension and resolution, *Mathematical Methods for Curves and Surfaces, Tromsø'2004*

(Ed-s: M. Dæhlen, K. Mørken, L. Schumaker), Nashboro Press, Brentwood, NC (2005), 103-114.

[6] L.T. Dechevsky, J. Gundersen, Scientific visualization for PDEs of 2nd order II: Comparative visualization of the Green's functions for elliptic, parabolic and hyperbolic cases, *International Journal of Pure and Applied Mathematics*, **41**, No. 9 (2007), 1261-1276.

[7] L.T. Dechevsky, J. Gundersen, Scientific visualization for PDEs of 2nd order III: Comparative visualization of solutions for elliptic, parabolic, hyperbolic and mixed-type cases, *International Journal of Pure and Applied Mathematics*, **41**, No. 9 (2007), 1277-1288.

[8] L.T. Dechevsky, J. Gundersen, Scientific visualization for PDEs of 2nd order IV: Comparison between the continual and the discrete boundary value problem, *International Journal of Pure and Applied Mathematics*, **41**, No. 9 (2007), 1289-1302.

[9] J. Gundersen, L.T. Dechevsky, Scientific visualization for the ODE-based simulator BedSim of LKAB, *International Journal of Pure and Applied Mathematics*, **41**, No. 9 (2007), 1197-1217.

[10] L. Hörmander, *The Analysis of Linear Partial Differential Operators, III, Pseudo-Differential Operators*, Springer, Berlin (1985).

[11] L. Hörmander, *The Analysis of Linear Partial Differential Operators, III*, Grundlehren der Mathematischen Wissenschaften, Fundamental Principles of Mathematical Sciences, **274**, Springer-Verlag, Berlin (1994); *Pseudo-Differential Operators*, Corrected Reprint of the 1985 original.

[12] K. Markov, *Mathematical Modelling*, Universitetska Biblioteka, **420**, Sofia University Publishing, Sofia (2002), In Bulgarian.

[13] B. Olsen, *Visualization of Complex-valued Functions of One Complex Variable*, M.Sc. Thesis (Supervisor: L.T. Dechevsky), Narvik University College (2004).

[14] M. Reed, B. Simon, *Methods of Modern Mathematical Physics, I*, Second Edition, Academic Press Inc., Harcourt Brace Jovanovich Publishers, New York (1980).

[15] A.A. Samarskii, *The Theory of Difference Schemes, Pure and Applied Mathematics*, Marcel Dekker Inc., New York (2001).

[16] I. Stakgold, *Boundary Problems of Mathematical Physics*, SIAM, **2**, Philadelphia (2000).

[17] A.N. Tikhonov, A.A. Samarskii, *Equations of Mathematical Physics*, Macmillan, Pergamon Press, New York (1963).

[18] Visualization (Graphic), Wikipedia Article, http://en.wikipedia.org/wiki/Scientific_visualization

Appendix A: The Parabolic Equation in Subsection 4.1

A.1 Proof of Formula (3) for the Green's function

First we will study problem (2) with homogeneous RHS and boundary conditions:

$$F(x,t) \equiv 0, \;\; u(0,t) \equiv 0, \;\; u(1,t) \equiv 0$$

By the Fourier method of separation of variables, we look for particular non-trivial solutions in tensor-product form

$$u(x,t) = X(x) \cdot T(t)$$

where X and T are real functions. From (2) we obtain:

$$T'(t) \cdot X(x) = X''(x) \cdot T(t)$$

$$\frac{X''(x)}{X(x)} = \frac{T'(t)}{T(t)} = \lambda$$

where λ must be a constant. This gives us the following two equations:

$$X''(x) - \lambda X(x) = 0 \tag{23}$$

$$T'(t) - \lambda T(t) = 0 \tag{24}$$

From the boundary conditions we get:

$$\left.\begin{array}{l} u(0,t) = X(0) \cdot T(t) = 0 \\ u(1,t) = X(1) \cdot T(t) = 0 \end{array}\right\} \Rightarrow X(0) = X(1) = 0. \tag{25}$$

This results in the Sturm-Liouville problem (23, 25). This problem has non-trivial solution only for some λ. More precisely, because X is a real-valued function, so is X$''$ and therefore λ is real.

For this problem we have the three following cases:

Case 1, $\lambda > 0$**:** The general solution of (23) is now

$$X(x) = C_1 e^{x\sqrt{\lambda}} + C_2 e^{-x\sqrt{\lambda}}$$

and $C_1,\ C_2$ must be such that the boundary conditions (25) are fulfilled, that is:

$$\left.\begin{array}{l} C_1 + C_2 = 0 \\ C_1 e^{\sqrt{\lambda}} + C_2 e^{-\sqrt{\lambda}} = 0 \end{array}\right\} \Rightarrow C_1 = C_2 = 0$$

because $\begin{vmatrix} 1 & 1 \\ e^{\sqrt{\lambda}} & e^{-\sqrt{\lambda}} \end{vmatrix} \neq 0.$

Case 2, $\lambda = 0$**:** The general solution of (23) is now of the form

$$X(x) = C_1 x + C_2$$

and from (25) yields

$$\left.\begin{array}{l} C_2 = 0 \\ C_1 + C_2 = 0 \end{array}\right\} \Rightarrow C_1 = C_2 = 0$$

Case 3, $\lambda < 0$**:** Denote

$$\lambda = -k^2, \tag{26}$$

where k is real. The general solution of (23) is now

$$X(x) = C_1 \cos(kx) + C_2 \sin(kx)$$

and (25) yields $C_1 = 0$, $C_2 \sin(k) = 0$, which have non-trivial solution if and only if $C_2 \neq 0$. Therefore $\sin(k) = 0$, hence $k = n\pi$, $n = 0, \pm 1, \pm 2, \ldots$.

From here we see that the only non-trivial solutions of (23, 25) of the prescribed type are

$$X_n(x) = C_n \sin(\pi n x), \quad n = 0, \pm 1, \pm 2, \ldots \tag{27}$$

with C_n being arbitrary constants such that $C_n \neq 0$. From (26) we also have that

$$\lambda = -\pi^2 n^2. \tag{28}$$

Next, we turn to (24) which is a first order linear ODE, with the general solution

$$T(t) = B \cdot e^{\lambda t} \tag{29}$$

where B is an arbitrary constant. From (28) and (29), we get all the possible non-trivial solutions of (29):

$$T_n(t) = B_n e^{-\pi^2 n^2 t}, \quad n = 0, \pm 1, \pm 2, \ldots \tag{30}$$

where B_n is an arbitrary constant such that $B_n \neq 0$.

Remark. It is enough to study (27-30) only for $n = 1, 2, \ldots$. Indeed, if $n = 0$, the solution is the trivial identical zero, which is of no interest. If $n = -1, -2, \ldots$, then $\sin(\pi n x) = -\sin(\pi(-n)x)$, with $-n = 1, 2, \ldots$, and the factor -1 is accounted for by the fact that C_n can be arbitrary. Therefore, from now on, we shall always assume $n = 1, 2, \ldots$ only.

By way of odd extension of the functions in $L_2[0, 1]$ to functions in $L_2[-1, 1]$, the orthogonal system

$$\{\sin(\pi n x), \;\; x \in [0, 1]\}_{n=1}^{\infty} \tag{31}$$

is an orthonormal basis of $L_2[0, 1]$, see [2] (the orthonormality is obtained by direct computation of the inner products $\int_0^1 \sin(\pi m x) \sin(\pi n x)$)

It then follows that $u(x, t)$ has the form:

$$\begin{aligned} u(x,t) &= \sum_{n=1}^{\infty} A_n T_n(t) \cdot X_n(x) \\ &= \sum_{n=1}^{\infty} A_n e^{-\pi^2 n^2 t} \cdot \sin(\pi n x) \end{aligned} \tag{32}$$

Next, let us study the case of homogeneous RHS and boundary conditions and inhomogeneous initial condition in (2):

$$F(x, t) \equiv 0, \;\; \psi^{(0)}(t) \equiv \psi^{(0)}(t) \equiv 0.$$

Requiring the fulfillment of the initial condition gives

$$u(x, 0) = \sum_{n=1}^{\infty} A_n \sin(\pi n x) = \varphi(x)$$

and, in view of (31),

$$A_n = 2 \int_0^1 \varphi(\xi) \cdot \sin(\pi n \xi) d\xi \tag{33}$$

From (32), (33), after changing order of summation and integration, we get $u(x, t) = \int_0^1 \mathrm{G}(x, \xi; t) \cdot \varphi(\xi) d\xi$ where

$$\mathrm{G}(x, \xi; t) = 2 \cdot \sum_{n=1}^{\infty} e^{-\pi^2 n^2 t} \cdot \sin(\pi n x) \cdot \sin(\pi n \xi), \tag{34}$$

which yields (3).

A.2 Proof of the Integral Representation (5) and (4) for Sufficiently Smooth Data

First, let us solve the case of homogeneous initial and boundary conditions $\varphi(x) \equiv 0$, $\psi^{(0)}(t) \equiv \psi^{(0)}(t) \equiv 0$ and inhomogeneous RHS $F(x,t)$. Now we seek the solution in the form

$$u(x,t) = \sum_{n=1}^{\infty} u_n(t) \cdot \sin(\pi n x) \tag{35}$$

with the following expansion of $F(x,t)$

$$F(x,t) = \sum_{n=1}^{\infty} f_n(t) \cdot \sin(\pi n x) \tag{36}$$

where

$$f_n(t) = 2 \cdot \int_0^1 F(\xi,t) \cdot \sin(\pi n \xi) d\xi \tag{37}$$

Plugging (35-37) into (2), we get

$$\sum_{n=1}^{\infty} \sin(\pi n x) \cdot \left(\pi^2 n^2 u_n(t) + \dot{u}(t) - f_n(t)\right) = 0 \tag{38}$$

for all x, t, and because the $\sin(\pi n x)$'s are linearly independent, (38) is equivalent to

$$\dot{u}_n(t) = -\pi^2 n^2 \cdot u_n(t) + f_n(t), \;\; n = 1, 2, \ldots, \text{ for all } t > 0. \tag{39}$$

Using the initial condition

$$u(x,0) = \sum_{n=1}^{\infty} u_n(0) \cdot \sin(\pi n x) = 0, \;\; \text{for all } x \in [0,1], \tag{40}$$

we get the initial conditions

$$u_n(0) = 0, \;\; n = 1, 2, \ldots. \tag{41}$$

Pairing (39) with (41) for every $n = 1, 2, \ldots$, we get an initial-value problem for 1st order linear ODE, which after computations (finding first the general solution of the homogeneous equation and then varying the constants by Lagrange's method) we arrive at

$$u_n(t) = \int_0^t e^{-\pi^2 n^2 (t-\tau)} f_n(\tau) d\tau. \tag{42}$$

Now plugging (42) into (35) gives, after changing the order of series sum-

mation and integration,

$$u(x,t) = \int_0^t \int_0^1 \mathrm{G}(x,\xi,t-\tau)\cdot F(\xi,\tau)d\xi d\tau \tag{43}$$

(This commutation is always possible for F smooth enough.)

Using the linearity of problem (2) we can now obtain the solution of (2) with inhomogeneous initial condition φ and RHS F, but still homogeneous boundary conditions, as follows:

$$\begin{aligned} u(x,t) = &\int_0^t \int_0^1 \mathrm{G}(x,\xi,t-\tau)\cdot F(\xi,\tau)d\xi d\tau \\ &+ \int_0^1 \mathrm{G}(x,\xi,t)\cdot\varphi(\xi)d\xi \end{aligned} \tag{44}$$

Next, we reduce the general case of inhomogeneous boundary condition, to the homogeneous case with solution (44). To this end, we write the solution of the inhomogeneous problem (2) as

$$u(x,t) = v(x,t) + (1-x)\cdot\psi^{(0)}(t) + x\cdot\psi^{(1)}(t) \tag{45}$$

and obtain from (2) and (45) that $v(x,t)$ is the solution of a new problem of type (2) with homogeneous boundary conditions $\bar{\psi}^{(0)}(t) = \bar{\psi}^{(1)}(t) = 0$, RHS of the form

$$\bar{F}(x,t) = F(x,t) - (1-x)\dot{\psi}^{(0)}(t) - x\dot{\psi}^{(1)}(t) \tag{46}$$

(assuming, for the moment, that $\psi^{(0)}$ and $\psi^{(1)}$ are sufficiently smooth, i.e., C^1 in t), and initial-value condition of the form,

$$\bar{\varphi}(x) = \varphi(x) - (1-x)\psi^{(0)}(0) - x\psi^{(1)}(0) \tag{47}$$

Then, (44-47) yield

$$\begin{aligned} v(x,t) = &\int_0^t \int_0^1 \mathrm{G}(x,\xi,t-\tau)\cdot\bar{F}(\xi,\tau)d\xi d\tau \\ &+ \int_0^1 \mathrm{G}(x,\xi,t)\cdot\bar{\varphi}(\xi)d\xi \end{aligned} \tag{48}$$

from where

$$u(x,t) = (1-x)\cdot\psi^{(0)}(t) + x\cdot\psi^{(1)}(t)$$

$$
\begin{aligned}
&+\int_0^1 \mathrm{G}(x,\xi;t)\cdot\Big[\varphi(\xi)-(1-\xi)\cdot\psi^{(0)}(0)+\xi\cdot\psi^{(1)}(0)\Big]d\xi\\
&+\int_0^t\int_0^1 \mathrm{G}(x,\xi;t-\tau)\cdot\left[F(\xi,\tau)-(1-\xi)\cdot\frac{\partial\psi^{(0)}}{\partial\tau}(\tau)+\xi\cdot\frac{\partial\psi^{(1)}}{\partial\tau}(\tau)\right]d\xi d\tau\\
&=\int_0^t\int_0^1 \mathrm{G}(x,\xi;t-\tau)\cdot F(\xi,\tau)d\xi d\tau\\
&+\int_0^1 \mathrm{G}(x,\xi;t)\cdot\varphi(\xi)d\xi\\
&+(1-x)\cdot\psi^{(0)}(t)-\int_0^t\int_0^1 G(x,\xi;t-\tau)\cdot(1-\xi)\cdot\frac{\partial\psi^{(0)}}{\partial\tau}(\tau)d\xi d\tau\\
&-\int_0^1 \mathrm{G}(x,\xi;t)\cdot(1-\xi)\cdot\psi^{(0)}(0)d\xi\\
&+x\cdot\psi^{(1)}(t)-\int_0^t\int_0^1 \mathrm{G}(x,\xi;t-\tau)\cdot\xi\cdot\frac{\partial\psi^{(1)}}{\partial\tau}(\tau)d\xi d\tau\\
&-\int_0^1 \mathrm{G}(x,\xi;t)\cdot\xi\cdot\psi^{(1)}(0)d\xi\,, \quad (49)
\end{aligned}
$$

which proves (5). Moreover, (49) yields

$$\begin{aligned} u(x,t) = &\int_0^t \int_0^1 G(x,\xi;t-\tau)\cdot F(\xi,\tau)d\xi d\tau \\ &+ \int_0^1 G(x,\xi;t)\cdot\varphi(\xi)d\xi \\ &+ \int_0^t \frac{\partial}{\partial\xi}G(x,0;t-\tau)\cdot\psi^{(0)}(\tau)d\tau \\ &- \int_0^t \frac{\partial}{\partial\xi}G(x,1;t-\tau)\cdot\psi^{(1)}(\tau)d\tau \end{aligned} \tag{50}$$

where

$$\frac{\partial}{\partial\xi}G(x,\xi;t-\tau) = 2\pi\cdot\sum_{n=1}^{\infty} n\cdot e^{-\pi^2n^2(t-\tau)}\sin(\pi nx)\cdot\cos(\pi n\xi),$$

$$\frac{\partial}{\partial\xi}G(x,0;t-\tau) = 2\pi\cdot\sum_{n=1}^{\infty} n\cdot e^{-\pi^2n^2(t-\tau)}\sin(\pi nx),$$

$$\frac{\partial}{\partial\xi}G(x,1;t-\tau) = 2\pi\cdot\sum_{n=1}^{\infty} (-1)^n\cdot n\cdot e^{-\pi^2n^2(t-\tau)}\sin(\pi nx),$$

which yields (4).

Remark In (49), (50) $G(x,\xi;t-\tau)$ and $G(x,\xi;\tau)$ are computed again via (34).

The proof that (49) is equivalent to (50) is given below, and is based on commuting the double integral $\int_0^t\int_0^1 = \int_0^1\int_0^t$, integration by parts in $\int_0^t$ and $\int_0^1$, and using the fact that $\frac{\partial}{\partial\tau}$G and $\frac{\partial^2}{\partial\xi^2}$G are related in a simple way by the PDE in (2).

A.2.1 Proof that (49) and (50) are Equivalent

In (49) we commute the integrals $\int_0^t\int_0^1 = \int_0^1\int_0^t$ (see also Section 5) and get:

$$\int_0^t \int_0^1 G(x,\xi;t-\tau)\cdot(1-\xi)\cdot\frac{\partial\psi^{(0)}}{\partial\tau}(\tau)d\xi d\tau$$

$$= \int_0^1 (1-\xi) \int_0^t G(x,\xi;t-\tau) \cdot \frac{\partial \psi^{(0)}}{\partial \tau}(\tau) d\tau d\xi = \int_0^1 (1-\xi)$$

$$\times \left[G(x,\xi;t-\tau) \cdot \psi^{(0)}(\tau) \Big|_{\tau=0}^{\tau=t} - \int_0^t \cdot \frac{\partial}{\partial \tau} \left[G(x,\xi;t-\tau) \right] \psi^{(0)}(\tau) d\tau \right] d\xi$$

$$= \int_0^1 (1-\xi) \Big(G(x,\xi;0) \cdot \psi^{(0)}(t) - G(x,\xi;t) \cdot \psi^{(0)}(0) \Big) d\xi$$

$$+ \int_0^1 (1-\xi) \int_0^t G_t(x,\xi;t-\tau) \cdot \psi^{(0)}(\tau) d\tau d\xi$$

$$= \psi^{(0)}(t) \int_0^1 (1-\xi) G(x,\xi;0) d\xi - \psi^{(0)}(0) \int_0^1 (1-\xi) G(x,\xi;t) d\xi$$

$$+ \int_0^t \psi^{(0)}(\tau) \int_0^1 (1-\xi) G_t(x,\xi;t-\tau) d\xi d\tau. \quad (51)$$

Now, compute explicitly $G_t(x,\xi;t-\tau)$ from the series expansion (34):

$$G_t(x,\xi;t-\tau) = -2 \sum_{n=1}^{\infty} \pi^2 n^2 e^{-\pi^2 n^2 (t-\tau)} \sin(\pi n x) \cdot \sin(\pi n \xi) \quad (52)$$

It is verified directly also that

$$G_{\xi\xi}(x,\xi;t-\tau) = -2 \sum_{n=1}^{\infty} \pi^2 n^2 e^{-\pi^2 n^2 (t-\tau)} \sin(\pi n x) \cdot \sin(\pi n \xi) \quad (53)$$

From (52) and (53) we get

$$G_t(x,\xi;t-\tau) = G_{\xi\xi}(x,\xi;t-\tau) \quad (54)$$

for all relevant x, ξ, t and τ (excluding the case $x=\xi$, $t=\tau$).

Plugging (54) into the last integral in (51) now yields, after integration by

parts in $\int_0^1 d\xi$:

$$\begin{aligned}
&\int_0^t \psi^{(0)}(\tau) \int_0^1 (1-\xi) G_t(x,\xi;t-\tau) d\xi d\tau \\
&= \int_0^t \psi^{(0)}(\tau) \int_0^1 (1-\xi) G_{\xi\xi}(x,\xi;t-\tau) d\xi d\tau \\
&= \int_0^t \psi^{(0)}(\tau) \left[(1-\xi) G_\xi(x,\xi;t-\tau)|_{\xi=0}^1 - \int_0^1 G_\xi(x,\xi;t-\tau) d(1-\xi) \right] d\tau \qquad (55) \\
&= \int_0^t \psi^{(0)}(\tau) \left[0 - G_\xi(x,0;t-\tau) + \int_0^1 G_\xi(x,\xi;t-\tau) d\xi \right] d\tau \\
&= -\int_0^t G_\xi(x,0;t-\tau)\psi^{(0)}(\tau) d\tau + \int_0^t \underbrace{G(x,1;t-\tau)}_{\substack{=0, \\ \text{because } \sin(\pi n)=0}} \psi^{(0)}(\tau) d\tau \\
&\qquad - \int_0^t \underbrace{G(x,0;t-\tau)}_{=0} \psi^{(0)}(\tau) d\tau \\
&= -\int_0^t G_\xi(x,0;t-\tau)\psi^{(0)}(\tau) d\tau
\end{aligned}$$

Returning back to (51), we note also that $\int_0^t G(x,\xi;0)\cdot\phi(\xi) = \phi(\xi)$ for every admissible ϕ, i.e,

$$G(x,\xi;0 = \sum_{n=0}^{\infty} \sin(\pi n x)\cdot\sin(\pi n \xi) = \delta(x-\xi) \qquad (56)$$

where convergence in (56) is in the topology of generalized functions (see, e.g., [14], Section 5.3).

Plugging (55) and (56) into (51), we get

$$\begin{aligned}
&\int_0^t \int_0^1 G(x,\xi;t-\tau)\cdot(1-\xi)\cdot\frac{\partial\psi^{(0)}}{\partial\tau}(\tau)d\xi d\tau \\
=&\psi^{(0)}(t)\int_0^1 (1-\xi)G(x,\xi;0)d\xi - \psi^{(0)}(0)\int_0^1 (1-\xi)G(x,\xi;t)d\xi \\
&-\int_0^t G_\xi(x,0;t-\tau)\psi^{(0)}(\tau)d\tau \qquad (57)\\
=&\psi^{(0)}(t)\cdot(1-x) - \psi^{(0)}(0)\int_0^1 (1-\xi)G(x,\xi;t)d\xi \\
&-\int_0^t G_\xi(x,0;t-\tau)\psi^{(0)}(\tau)d\tau
\end{aligned}$$

In analogous way we get from (49)

$$\begin{aligned}
&\int_0^t \int_0^1 G(x,\xi;t-\tau)\cdot\xi\cdot\frac{\partial\psi^{(1)}}{\partial\tau}(\tau)d\xi d\tau \\
&\qquad = \psi^{(1)}(t)\cdot x - \psi^{(1)}(0)\int_0^1 \xi\cdot G(x,\xi;t)d\xi \\
&\qquad\qquad -\int_0^t G_\xi(x,1;t-\tau)\psi^{(1)}(\tau)d\tau\,. \qquad (58)
\end{aligned}$$

Plugging (57) and (58) into (49) we obtain, after appropriate cancellation of terms, (50), which proves that (49) = (50) ((5) and (4)). For non-smooth $\psi^{(0)}$ and $\psi^{(1)}$, see Section 5.

Appendix B: The Hyperbolic Equation in Subsection 4.2

B.1 Proof of Formula (7) for the Green's Function

Using the Fourier method of separation as in Subsection 5, we get the following two equations:

$$X''(x) - \lambda X(x) = 0 \tag{59}$$

$$T''(t) - \lambda T(t) = 0 \tag{60}$$

This problem is of the same type as (23), but for the scaled interval $[0, T]$. There is also a difference in the boundary conditions (25) which are now not directly available (see the two initial-value conditions)

From the derivation of (26) we already know the possible values for λ, and from (60) we find the following general solution:

$$T_n(t) = A_n \cos\left(\tfrac{\pi n t}{T}\right) + B_n \sin\left(\tfrac{\pi n t}{T}\right) \tag{61}$$

for $n = 1, 2, \ldots$.

From (27) we have that $X_n(x) = C_n \dot{\sin}(\pi n x)$ implying that $u(x, t)$ is of the form

$$u(x,t) = \sum_{n=1}^{\infty} \left(A_n \cos\left(\tfrac{\pi n t}{T}\right) + B_n \sin\left(\tfrac{\pi n t}{T}\right)\right) \cdot \sin(\pi n x) \tag{62}$$

Now we can find A_n and B_n from (62) and the initial conditions (again, for sufficiently smooth data it can be shown that the RHS is uniformly convergent together with its derivative, so that the series at the RHS of (62) can be differentiated.)

$$u(x,0) = \varphi^{(0)}(x) = \sum_{n=1}^{\infty} A_n \cdot \sin(\pi n x), \tag{63}$$

$$u_t(x,0) = \varphi^{(1)}(x) = \sum_{n=1}^{\infty} B_n \frac{\pi n}{T} \sin(\pi n x) \tag{64}$$

where $x \in [0, 1]$. In view of the orthonormality of the basis $\{\sin(\pi n x),\ x \in [0,1]\}_{n=1}^{\infty}$ on $L_2[0, 1]$, see (31), we get:

$$\begin{aligned} A_n &= 2\int_0^1 \varphi^{(0)}(x)\cdot\sin(\pi n x)dx \\ B_n &= \tfrac{2T}{\pi n}\int_0^1 \varphi^{(1)}(x)\cdot\sin(\pi n x)dx \end{aligned} \tag{65}$$

From (62) and (65), after changing the order of summation and integration we get:

$$u(x,t) = \int_0^1 G_t\left(x,\xi;t\right)\varphi^{(0)}(\xi)d\xi + \int_0^1 G\left(x,\xi;t\right)\varphi^{(1)}(\xi)d\xi \tag{66}$$

where

$$G\left(x,\xi;t\right) = \frac{2T}{\pi}\sum_{n=1}^{\infty}\frac{1}{n}\cdot\sin\left(\frac{\pi n t}{T}\right)\cdot\sin\left(\pi n x\right)\cdot\sin\left(\pi n\xi\right) \tag{67}$$

$$G_t\left(x,\xi;t\right) = 2\sum_{n=1}^{\infty}\cos\left(\frac{\pi n t}{T}\right)\cdot\sin\left(\pi n x\right)\cdot\sin\left(\pi n\xi\right) \tag{68}$$

B.2 Proof of the Integral Representation (9) and (8) for Sufficiently Smooth Data

Now considering the case of homogeneous initial and boundary conditions and inhomogeneous RHS, we derive the same equations, as with the parabolic equations, see (35), (36) and (37). Plugging them into (6) yields:

$$\sum_{n=1}^{\infty}\sin\left(\pi n x\right)\left(\pi^2 n^2 u_n(t) + \ddot{u}_n(t) - f_n(t)\right) = 0 \tag{69}$$

where we have:

$$\varphi^{(0)}(x) = \sum_{n=1}^{\infty}\alpha_n\sin(\pi n x) \tag{70}$$

$$\alpha_n = 2\int_0^1 \varphi^{(0)}(\xi)\sin(\pi n\xi)d\xi \tag{71}$$

$$\varphi^{(1)}(x) = \sum_{n=1}^{\infty}\beta_n\sin(\pi n x) \tag{72}$$

$$\beta_n = 2\int_0^1 \varphi^{(1)}(\xi)\sin(\pi n\xi)d\xi \tag{73}$$

Hence, for every $n = 1, 2, \ldots$, we get the following initial value problem for second order ODE:

$$\ddot{u}_n(t) + \pi^2 n^2 u_n(t) = f_n(t), \quad t \in [0, T] \tag{74}$$

$$u_n(0) = \alpha_n \tag{75}$$

$$\dot{u}_n(0) = \beta_n \tag{76}$$

where the conditions (75) and (76) are obtained in the same way as (65).

Next, we obtain in the same way (this time we have included also inhomogeneous initial conditions, which does not change the method of proof here) as for (42) in the parabolic case,

$$\begin{aligned} u_n(t) = &\frac{T}{\pi n}\int_0^t \sin\left(\frac{\pi n(t-\tau)}{T}\right) f_n(t)d\tau \\ &+ \alpha_n \cos\left(\frac{\pi n t}{T}\right) + \frac{T}{\pi n}\beta_n \sin\left(\frac{\pi n t}{T}\right) \end{aligned} \tag{77}$$

and by using the linearity of problem (6) in the same way as for the parabolic case, we obtain the solution of (6) with inhomogeneous initial conditions $\varphi^{(0)}$ and $\varphi^{(1)}$, and RHS F, but still homogeneous boundary conditions, as follows;

$$\begin{aligned} u(x,t) = &\int_0^t \int_0^1 G\left(x,\xi;t-\tau\right)\cdot F\left(\xi,\tau\right)d\xi d\tau \\ &+ \int_0^1 G_t\left(x,\xi;t\right)\cdot\varphi^{(0)}\left(\xi\right)d\xi + \int_0^1 G\left(x,\xi;t\right)\cdot\varphi^{(1)}\left(\xi\right)d\xi \end{aligned}$$

where $G(x, \xi; t-\tau)$ is computed via (67)

Finally, we reduce the solution of the problem with inhomogeneous boundary conditions to the case with homogeneous ones. We write the solution of the inhomogeneous problem as

$$u(x,t) = v(x,t) + (1-x)\psi^{(0)}(t) + x\psi^{(1)}(t) \tag{78}$$

and obtain from (78) that $v(x,t)$ is the solution of a new problem with homogeneous boundary conditions $\bar{\psi}^{(0)}(t) \equiv \bar{\psi}^{(1)}(t) \equiv 0$, RHS of the form

$$\bar{F}(x,t) = F(x,t) - (1-x)\ddot{\psi}^{(0)}(t) - x\ddot{\psi}^{(1)}(t) \tag{79}$$

(assuming, for the moment, that $\psi^{(0)}$ and $\psi^{(1)}$ are C^2 in t - an assumption

which can be weakened considerably), and initial value conditions of the form:

$$\bar{\varphi}^{(0)}(x) = \varphi^{(0)}(x) - (1-x)\psi^{(0)}(0) - x\psi^{(1)}(0) \tag{80}$$

$$\bar{\varphi}^{(1)}(x) = \varphi^{(1)}(x) - (1-x)\dot{\psi}^{(0)}(0) - x\dot{\psi}^{(1)}(0) \tag{81}$$

then (48) yield

$$\begin{aligned} v(x,t) = &\int_0^t \int_0^1 G\left(x,\xi;t-\tau\right)\cdot \bar{F}\left(\xi,\tau\right) d\xi d\tau \\ &+ \int_0^1 G_t\left(x,\xi;t\right)\cdot \bar{\varphi}^{(0)}\left(\xi\right) d\xi + \int_0^1 G\left(x,\xi;t\right)\cdot \bar{\varphi}^{(1)}\left(\xi\right) d\xi, \end{aligned} \tag{82}$$

which proves (9). To obtain the proof of (8) from here, we first note that (49) now becomes

$$\begin{aligned} u(x,t) = &(1-x)\psi^{(0)}(t) + x\psi^{(1)}(t) \\ &+ \int_0^1 G_t(x,\xi;t)\left[\varphi^{(0)}(\xi) - (1-\xi)\psi^{(0)}(0) - \xi\psi^{(1)}(0)\right]d\xi \\ &+ \int_0^1 G(x,\xi;t)\left[\varphi^{(1)}(\xi) - (1-\xi)\dot{\psi}^{(0)}(0) - \xi\dot{\psi}^{(1)}(0)\right]d\xi \\ &+ \int_0^t \int_0^1 G(x,\xi;t-\tau)\left[F(\xi,\tau) - (1-\xi)\ddot{\psi}^{(0)}(\tau) - \xi\ddot{\psi}^{(1)}(\tau)\right]d\xi d\tau \\ &= \int_0^t \int_0^1 G(x,\xi;t-\tau)F(\xi,\tau)d\xi d\tau \\ &+ \int_0^1 G_t(x,\xi;t)\varphi^{(0)}(\xi)d\xi + \int_0^1 G(x,\xi;t)\varphi^{(1)}(\xi)d\xi \\ &+ (1-x)\psi^{(0)}(t) - \int_0^t \int_0^1 G(x,\xi;t-\tau)(1-\xi)\ddot{\psi}^{(0)}(\tau)d\xi d\tau \\ &- \int_0^1 G(x,\xi;t)(1-\xi)\dot{\psi}^{(0)}(0)d\xi - \int_0^1 G_t(x,\xi;t)(1-\xi)\psi^{(0)}(0)d\xi \end{aligned}$$

$$+ x\psi^{(1)}(t) - \int_0^t \int_0^1 G(x,\xi;t-\tau)\xi\ddot{\psi}^{(1)}(\tau)d\xi d\tau$$

$$- \int_0^1 G(x,\xi;t)\xi\dot{\psi}^{(1)}(0)d\xi - \int_0^1 G_t(x,\xi;t)\xi\psi^{(1)}(0)d\xi = (R_1)\,. \quad (83)$$

By integration by parts two times in $\int_0^t d\tau$ we get:

$$-\int_0^t \int_0^1 G(x,\xi;t-\tau)(1-\xi)\ddot{\psi}^{(0)}(\tau)d\xi d\tau =$$

$$= -\int_0^1 (1-\xi)\Big[G(x,\xi;0)\dot{\psi}^{(0)}(t) - G(x,\xi;t)\dot{\psi}^{(0)}(0) + G_t(x,\xi;0)\psi^{(0)}(t)$$

$$- G_t(x,\xi;t)\psi^{(0)}(0) + \int_0^t G_{tt}(x,\xi;t-\tau)\psi^{(0)}(\tau)d\tau\Big]\, d\xi = (R_2)$$

We have from (67) (for simplicity we assume here that $T=1$)

$$\begin{aligned} G_{tt}(x,\xi;t-\tau) &= -2\pi\sum_{n=1}^{\infty} n\sin(\pi n(t-\tau))\sin(\pi n x)\sin(\pi n\xi) \\ &= G_{\xi\xi}(x,\xi;t-\tau) \end{aligned} \quad (84)$$

(here we skip the discussion of the conditions under which it is possible to differentiate the series $\sum_{n=1}^{\infty}$), therefore,

$$(R_2) = -\dot{\psi}^{(0)}(t)\int_0^1 (1-\xi)G(x,\xi;0)d\xi + \dot{\psi}^{(0)}(0)\int_0^1 (1-\xi)G(x,\xi;t)d\xi$$

$$- \psi^{(0)}(t)\int_0^1 (1-\xi)G_t(x,\xi;0)d\xi + \psi^{(0)}(0)\int_0^1 (1-\xi)G_t(x,\xi;t)d\xi$$

$$- \int_0^t \psi^{(0)}(\tau)\int_0^1 (1-\xi)G_{\xi\xi}(x,\xi;t-\tau)d\xi d\tau$$

$$= -\dot{\psi}^{(0)}(t)\int_0^1 (1-\xi)G(x,\xi;0)d\xi - \psi^{(0)}(t)\int_0^1 (1-\xi)G_t(x,\xi;0)d\xi$$

$$- \int_0^t \psi^{(0)}(\tau) \left[0 - G_\xi(x,0;t-\tau) + G(x,1;t-\tau) - G(x,0;t-\tau)\right] d\tau \,. \quad (85)$$

Analogously,

$$- \int_0^t \int_0^1 G(x,\xi;t-\tau)\xi\psi^{(1)}(\tau) d\xi d\tau =$$

$$= -\dot{\psi}^{(1)}(t) \int_0^1 \xi G(x,\xi;0) d\xi - \psi^{(1)}(t) \int_0^1 \xi G_t(x,\xi;0) d\xi$$

$$- \int_0^t \psi^{(1)}(\tau) \left[G_\xi(x,1;t-\tau) - 0 - G(x,1;t-\tau) + G(x,0;t-\tau)\right] d\tau \,. \quad (86)$$

Substituting (85) and (86) in (83), we get

$$(R_1) = (1-x)\psi^{(0)}(t) + x\psi^{(1)}(t) + \int_0^t \int_0^1 G(x,\xi;t-\tau)F(\xi,\tau) d\xi d\tau$$

$$+ \int_0^1 G_t(x,\xi;t)\varphi^{(0)}(\xi) d\xi + \int_0^1 G(x,\xi;t)\varphi^{(1)}(\xi) d\xi$$

$$- \dot{\psi}^{(0)}(t) \int_0^1 (1-\xi) G(x,\xi;0) d\xi - \psi^{(0)}(t) \int_0^1 (1-\xi) G_t(x,\xi;0) d\xi$$

$$+ \int_0^t \psi^{(0)}(\tau) G_\xi(x,0;t-\tau) d\tau - \int_0^t \psi^{(0)}(\tau) \left(G(x,1;t-\tau) - G(x,0;t-\tau)\right) d\tau$$

$$- \dot{\psi}^{(1)}(t) \int_0^1 \xi G(x,\xi;0) d\xi - \psi^{(1)}(t) \int_0^1 \xi G_t(x,\xi;0) d\xi$$

$$- \int_0^t \psi^{(1)}(\tau) G_\xi(x,1;t-\tau) d\tau + \int_0^t \psi^{(1)}(\tau) \left(G(x,1;t-\tau) - G(x,0;t-\tau)\right) d\tau$$

$$= (1-x)\psi^{(0)}(t) + x\psi^{(1)}(t) + \int_0^t \int_0^1 G(x,\xi;t-\tau)F(\xi,\tau) d\xi d\tau$$

$$+\int_0^1 G_t(x,\xi;t)\varphi^{(0)}(\xi)d\xi+\int_0^1 G(x,\xi;t)\varphi^{(1)}(\xi)d\xi$$
$$+\int_0^t G_\xi(x,0;t-\tau)\psi^{(0)}(\tau)d\tau+\int_0^t G_\xi(x,1;t-\tau)\psi^{(1)}(\tau)d\tau$$
$$+\int_0^t \left(\psi^{(1)}(\tau)-\psi^{(0)}(\tau)\right)\left(G(x,1;t-\tau)-G(x,0;t-\tau)\right)d\tau$$
$$-\int_0^1 \Big\{G(x,\xi;0)\left[(1-\xi)\dot{\psi}^{(0)}(t)+\xi\dot{\psi}^{(1)}(t)\right]+$$
$$+\,G_t(x,\xi;0)\left[(1-\xi)\psi^{(0)}(t)+\xi\psi^{(1)}(t)\right]\Big\}d\xi\,. \quad (87)$$

where (67) holds (we keep assuming $T=1$), hence

$$G(x,1;t-\tau)\equiv G(x,0;t-\tau)\equiv G(x,\xi;0)\equiv 0 \quad (88)$$

and

$$G_t(x,\xi;0)=2\sum_{n=1}^{\infty}\sin(\pi nx)\sin(\pi n\xi)=\delta(x,\xi) \quad (89)$$

hence,

$$\begin{aligned}u(t)=&\int_0^t\int_0^1 G(x,\xi;t-\tau)\cdot F(\xi,\tau)\,d\xi d\tau\\&+\int_0^1 G_t(x,\xi;t)\cdot\varphi^{(0)}(\xi)\,d\xi+\int_0^1 G(x,\xi;t)\cdot\varphi^{(1)}(\xi)\,d\xi\\&+\int_0^t G_\xi(x,0;t-\tau)\cdot\psi^{(0)}(\tau)\,d\tau-\int_0^1 G_\xi(x,1;t-\tau)\cdot\psi^{(1)}(\tau)\,d\tau\end{aligned} \quad (90)$$

which proves (8)

Appendix C: The Elliptic Equation in Subsection 4.3

C.1 Formula (11) for the Green's Function

The derivation of (12) has been outlined, e.g., in [16], Section 6.7, the derivation of (6.117). The full detail of this derivation can be recovered along the same lines as in Appendix 5 and will not be given explicitly here.

C.2 Proof of the Integral Representation (13) and (12) for Sufficiently Smooth Data

Next, we reduce the problem with inhomogeneous boundary conditions to the problem with homogeneous boundary conditions and modified RHS and initial value conditions as (79), (80) and (81). In the elliptic case we write the solution of the inhomogeneous problem as

$$u(x,t) = v(x,t) + (1-x)\cdot\psi^{(0)}(t) + x\cdot\psi^{(1)}(t) + \varphi^{(0)}(x)\cdot\frac{T-t}{T} + \varphi^{(1)}(x)\cdot\frac{t}{T} - \rho(x,t),$$

where

$$v(x,t) = \int_0^t\int_0^1 G\left(x,\xi;t,\tau\right)\cdot\bar{F}\left(\xi,\tau\right)d\xi d\tau + \int_0^1 G_t\left(x,\xi;t,0\right)\cdot\bar{\varphi}^{(0)}(\xi)d\xi + \int_0^1 G\left(x,\xi;t,0\right)\cdot\bar{\varphi}^{(1)}(\xi)d\xi, \quad (91)$$

with

$$\begin{aligned}
\bar{F}(\xi,\tau) =& F(\xi,\tau) - (1-\xi)\cdot\ddot{\psi}^{(0)}(\tau) - \xi\cdot\ddot{\psi^{(1)}}(\tau) \\
&- \left(\frac{T-\tau}{T}\right)\cdot\varphi''^{(0)}(\xi) - \frac{\tau}{T}\cdot\varphi''^{(1)}(\xi), \\
\bar{\varphi}^{(0)}(\xi) =& -(1-\xi)\cdot\psi^{(0)}(0) - \xi\cdot\psi^{(1)}(0) + \rho(\xi,0), \\
\bar{\varphi}^{(1)}(\xi) =& -(1-\xi)\cdot\psi^{(0)}(T) - \xi\cdot\psi^{(1)}(T) + \rho(\xi,T),
\end{aligned}$$

$$\rho(\xi,\tau) = \sum_{\mu=0}^{1}\sum_{\nu=0}^{1} u(\xi_\mu\tau_\nu)b_\mu(\xi)b_\nu(\tau)$$

$$= u(0,0)\cdot(1-\xi)\cdot\left(\frac{T-\tau}{T}\right) + u(0,T)\cdot(1-\xi)\cdot\frac{\tau}{T}$$
$$+ u(1,0)\cdot\xi\cdot\left(\frac{T-\tau}{T}\right) + u(1,T)\cdot\xi\cdot\frac{\tau}{T}.$$

from where (13) follows in the same way as formula (9) for the hyperbolic equation. The derivation of (12) from (13) is done along the lines of the derivation of (8) from (9) for the hyperbolic equation, and, therefore, will not be repeated explicitly here.

Appendix D: Finite Difference Scheme for the Parabolic Equation

D.1 Proof of Formulae (15) and (16) for the Discrete Green's Function

In our search for an explicit solution of (14) we first solve the homogeneous problem using a discrete Green's function. Then we reduce the inhomogeneous problem to a homogeneous problem.

We now consider the following discrete homogeneous problem:

$$\frac{w_{ij+1}-w_{ij}}{\tau} - \left(\sigma\frac{w_{i+1j+1}-2w_{ij+1}+w_{i-1j+1}}{h^2} + (1-\sigma)\frac{w_{i+1j}-2w_{ij}+w_{i-1j}}{h^2}\right) = f_{ij}$$

$$\begin{aligned} &i=1,2,\ldots,N-1, \quad j=0,1,2,\ldots,M-1 \\ &w_{i0}=\phi_i\equiv 0, && i=0,1,\ldots,N \\ &w_{0j}=\psi_j^{(0)}\equiv 0,\ w_{Nj}=\psi_j^{(1)}\equiv 0, && j=0,1,\ldots,M \end{aligned} \tag{92}$$

where $f_{ij}\equiv 0$ and the discrete consistency conditions $\phi_0 = w_{00} = \psi_0^0$, $\phi_N = w_{N0} = \psi_0^1$ are automatically fulfilled.

Using the method of separation of variables, we find the solution to (92), $w_{ij} = X_i T_j$. If we use a composition of left and right difference, equation (92) can be written, as follows:

$$\begin{aligned} &T_{t,j}X - (\sigma T_{j+1} + (1-\sigma)T_j)X_{\bar{x}x} = 0 \\ &X_iT_0 = 0, \quad i=0,1,\ldots,N, && \Rightarrow T_0 = 0 \\ &X_0T_j = 0, \quad X_NT_j = 0, \quad j=0,1,\ldots,M, && \Rightarrow X_0 = X_N = 0 \end{aligned}$$

This gives us

$$\Rightarrow \frac{T_{t,j}}{\sigma T_{j+1} + (1-\sigma)T_j} = \frac{X_{\bar{x}x}}{X} = \lambda$$

where λ must be a constant. We then get two separable differential equations:

$$\begin{aligned} X_{\bar{x}x} &= \lambda X && , X_0 = X_N = 0 \\ T_j &= \lambda\sigma\hat{T} + (1-\sigma)T_j && , T_0 = 0 \end{aligned}$$

These two equations will always have a trivial solution, but it is only the non-trivial solutions of the difference problems that is of any interest here;

1. $T_j = \lambda\sigma\hat{T} + (1-\sigma)T_j \ , T_0 = 0$
   The solution is similar to the solution of the differential problem:
   $$y'(t) - \lambda y(t) = 0, y(0) = 0,$$
   that only gives a trivial solution.
2. $X_{\bar{x}x} = \lambda X \ , X_0 = X_N = 0$
   We are now only searching for the non-trivial solutions. By the same reasoning as with the continual problem (23, 24), λ must be a negative number and we will get this difference problem:
   $$X_{\bar{x}x} - \lambda X = 0, \quad X_0 = X_N = 0$$
   with $x = ih$, $0 < i < N$, $h = \frac{1}{N}$ and $X(x) \neq 0$
   Written in the index form we have
   $$X_{i+1} - 2(1 - \frac{1}{2}h^2\lambda)X_i + X_{i-1} = 0, \quad i = 1, 2, \ldots, N-1$$
   We look for a solution in the form
   $$X(x) = A\sin(\alpha x)$$
   with A and α to be determined.
   We then have
   $$X_{i+1} + X_{i-1} = A\sin\alpha(x+h) + A\sin\alpha(x-h) = 2A\sin\alpha x\cos\alpha h$$
   Substituting into the index expansion:
   $$2A\sin\alpha x\cos(\alpha h) = 2A(1 - \frac{1}{2}h^2\lambda)\sin\alpha x$$
   Since we are only looking for the non-trivial solution, $\sin(\alpha x) \neq 0$, it then follows
   $$1 - \frac{1}{2}h^2\lambda = \cos(\alpha h)$$
   and
   $$\lambda = \frac{2}{h^2}(1 - \cos(\alpha h)) = \frac{4}{h^2}\sin^2\left(\frac{\alpha h}{2}\right)$$

We choose α in such a way that $X(x) = A\sin(\alpha x)$ satisfies the boundary conditions $X(0) = X(1) = 0$

The boundary conditions at the point $x = 0$ is automatically fulfilled for any α. At the point $x = 1$ we have $\sin\alpha = 0$ giving $\alpha = \alpha_\nu = \nu\pi$, $\nu = 1, 2, \ldots, N-1$

This gives us

$$\lambda_\nu = \frac{4}{h^2}\sin^2\left(\frac{\pi\nu h}{2}\right) = \frac{4}{h^2}\sin^2\left(\frac{\pi x_\nu}{2}\right) \tag{93}$$

$$X_\nu = A\sin(\pi\nu x_i) \tag{94}$$

where $A = \sqrt{2}$.

We may also assume for f_{ij} (which is defined only for $i = 1, \ldots, N-1$) that $f_{0j} \equiv f_{Nj} \equiv 0$, $j = 0, 1, \ldots, M$. Now we can solve the problem with arbitrary right-hand side f_{ij} and homogeneous boundary conditions ($\psi_j^{(0)} \equiv \psi_j^{(1)} \equiv 0$, $j = 0, 1, \ldots, M$), where the initial condition does not have to be homogeneous, because of the homogeneity of the boundary conditions and the consistency conditions at the corners, $\phi_0 = \phi_N = 0$.

Expanding ϕ_i in the basis X_ν, we have

$$\phi_i = \sum_{\nu=1}^{N-1} c_\nu X_\nu(x_i), \quad \text{where } c_\nu = \sum_{n=1}^{N-1} h\phi_n X_\nu(x_n) \tag{95}$$

in the same way,

$$f_{ij} = \sum_{\nu=1}^{N-1} b_{\nu j} X_\nu(x_i), \quad \text{where } b_{\nu j} = \sum_{n=1}^{N-1} h f_{nj} X_\nu(x_n) \tag{96}$$

$$w_{ij} = \sum_{\nu=1}^{N-1} a_{\nu j} X_\nu(x_i) \tag{97}$$

Now, plugging (95), (96) and (97) into (92) (with $\psi_j^{(0)} \equiv \psi_j^{(1)} \equiv 0$), we then get the following:

$$\frac{w_{ij+1} - w_{ij}}{\tau} - \left(\sigma\frac{w_{i+1j+1} - 2w_{ij+1} + w_{i-1j+1}}{h^2} + (1-\sigma)\frac{w_{i+1j} - 2w_{ij} + w_{i-1j}}{h^2}\right) = f_{ij},$$

hence,

$$\frac{1}{\tau}\sum_{\nu=1}^{N-1}(a_{\nu j+1} - a_{\nu j})X_\nu(x_i)$$

$$-\frac{1}{h^2}\left[(\sigma a_{\nu j+1}+(1-\sigma)a_{\nu j})(X_\nu(x_{i+1})-2X_\nu(x_i)+X_\nu(x_{i-1}))\right]$$
$$=\sum_{\nu=1}^{N-1} b_{\nu j}X_\nu(x_i)$$
$$i=1,2,\ldots,N-1,\quad j=0,1,\ldots,M-1.$$

The initial condition is

$$\begin{aligned} w_{i0} &= \phi_i \\ \sum_{\nu=1}^{N-1} a_{\nu 0}X_\nu(x_i) &= \sum_{\nu=1}^{N-1} c_\nu X_\nu(x_i),\quad i=1,2,\ldots,N-1. \end{aligned}$$

The boundary conditions are

$$w_{0j}=\psi_j^{(0)}=0,\quad w_{Nj}=\psi_j^{(1)}=0$$
$$\sum_{\nu=1}^{N-1} a_{\nu j}X_\nu(0)\equiv 0\equiv\sum_{\nu=1}^{N-1} a_{\nu j}X_\nu(1).$$

Then, commuting appropriately the summands we finally get the explicit solution of (92) in the form

$$w_{ij}=\sum_{\nu=1}^{N-1} h\Gamma_{ij}^{\nu}\phi_\nu+\sum_{\mu=0}^{j-1}\sum_{\nu=1}^{N-1} h\tau G_{ij}^{\nu\mu}f_{\nu\mu} \tag{98}$$

where

$$G_{ij}^{\nu\mu} = \sum_{n=1}^{N-1}\frac{1}{1+\lambda_n\tau\sigma}\left(1-\frac{\lambda_n\tau}{1+\lambda_n\tau\sigma}\right)^{j-\mu-1}X_n(x_\nu)X_n(x_i) \tag{99}$$

$$\Gamma_{ij}^{\nu} = \sum_{n=1}^{N-1}\left(1-\frac{\lambda_n\tau}{1+\lambda_n\tau\sigma}\right)^{j}X_n(x_\nu)X_n(x_i) \tag{100}$$

which proves (15) and (16).

D.2 Proof of the Explicit Sum Representation of the Solution in (17)

We have now found the solution for the case with homogeneous boundary conditions. Now we want to convert the inhomogeneous problem (14) into a problem with homogeneous boundary conditions and a new right-hand side f. This is relatively easy to do because of the linearity of the problem. Using a linear

approximation of the boundary conditions we can write the explicit solution of (14) as

$$V_{ij} = w_{ij} + (1 - x_i)\psi_j^{(0)} + x_i\psi_j^{(1)} \tag{101}$$

Substituting this into (14), we get

$$\frac{w_{ij+1} - w_{ij}}{\tau} - \left(\sigma\frac{w_{i+1j+1} - 2w_{ij+1} + w_{i-1j+1}}{h^2} + (1-\sigma)\frac{w_{i+1j} - 2w_{ij} + w_{i-1j}}{h^2}\right) = f_{ij} - \frac{(1-x_i)\left(\psi_{j+1}^{(0)} - \psi_j^{(0)}\right) + x_i\left(\psi_{j+1}^{(1)} - \psi_j^{(1)}\right)}{\tau}$$

Now we set

$$F_{ij} = f_{ij} - \frac{(1-x_i)\left(\psi_{j+1}^{(0)} - \psi_j^{(0)}\right) + x_i\left(\psi_{j+1}^{(1)} - \psi_j^{(1)}\right)}{\tau}$$

and convert the initial condition

$$V_{i0} = w_{i0} + (1-x_i)\psi_0^{(0)} + x_i\psi_0^{(1)} = \phi_i$$

$$\Rightarrow w_{i0} = \phi_i - (1-x_i)\psi_0^{(0)} - x_i\psi_0^{(1)} = \Phi_i,$$

and boundary conditions

$$\begin{aligned} V_{0j} &= w_{0j} + (1-x_0)\psi_j^{(0)} + x_0\psi_j^{(1)} = \psi_j^{(0)} \\ &\Rightarrow w_{0j} = \psi_j^{(0)} - \psi_j^{(0)} + x_0\psi_j^{(0)} - x_0\psi_j^{(1)} = \underbrace{x_0}_{=0}\left(\psi_j^{(0)} - \psi_j^{(1)}\right) = 0. \end{aligned}$$

$$\begin{aligned} V_{Nj} &= w_{Nj} + (1-x_N)\psi_j^{(0)} + x_N\psi_j^{(1)} = \psi_j^{(1)} \\ &\Rightarrow w_{Nj} = \psi_j^{(1)} - \psi_j^{(0)} + \underbrace{x_N}_{=1}\psi_j^{(0)} + \underbrace{x_N}_{=1}\psi_j^{(1)} = 0 \end{aligned}$$

we see that we have converted the inhomogeneous problem (14) into a problem with homogeneous boundary conditions.

We then have this explicit solution of (14)

$$\begin{aligned} V_{ij} &= w_{ij} + (1-x_i)\psi_j^{(0)} + x_i\psi_j^{(1)} \\ &= \sum_{\nu=1}^{N-1} h\Gamma_{ij}^{\nu}\Phi_\nu + \sum_{\mu=0}^{j-1}\sum_{\nu=1}^{N-1} h\tau G_{ij}^{\nu\mu}F_{\nu\mu} + (1-x_i)\psi_j^{(0)} + x_i\psi_j^{(1)} \end{aligned} \tag{102}$$

where

$$\begin{aligned} F_{ij} &= f_{ij} - \frac{(1-x_i)\left(\psi_{j+1}^{(0)} - \psi_j^{(0)}\right) + x_i\left(\psi_{j+1}^{(1)} - \psi_j^{(1)}\right)}{\tau} \\ \Phi_i &= \phi_i - (1-x_i)\psi_0^{(0)} - x_i\psi_0^{(1)} \end{aligned}$$

which proves (17).